JOURNAL OF MATERIALS SCIENCE 25 (1990) 1444–1454

Micron-scale indentation of amorphous and drawn PET surfaces

R. H. ION, H. M. POLLOCK
Department of Physics, University of Lancaster, Lancaster, England LA1 4YB
C. ROQUES-CARMES
E.N.S. of Mechanics and Microtechniques (ENSMM), 25030 Besançon, France

The plastic, elastic and flow properties of the near-surface region of poly(ethylene terephthalate), either amorphous or uniaxially drawn, are measured by means of a sub-microindentation technique with continuous depth recording. The depths investigated range from 0.2 to 6 μm. The drawn material is harder, with a larger value of elastic recovery parameter and a depth-load characteristic that indicates a departure from typical bulk behaviour. From "slow loading" tests, values of plasticity indices and of Young's modulus are derived. In "abrupt loading" tests the total recoverable deformation is greater: at depths less than 300 nm the behaviour is pseudo-plastic, while at greater depths the deformation is dominated by a Chasset-type anelastic compliance.

1. Introduction

Poly(ethylene terephthalate), or PET, is one of the linear saturated polymers which were first synthesized in the 1940s and is now known by many different trade names including "Mylar" and Terylene". Its uses have proved manifold, ranging from clothing to capacitors: recently much interest has been shown in its use as a base for magnetic tapes [1] where its suitability is due to the stiff polymer chain and resilient inter-chain bonds which prevent stretching and resultant data loss.

Plastics are often modified by the use of fillers to change both the mechanical and electrical properties; the list of additives is extensive and the processing techniques numerous. Thus, samples of PET from different sources may well possess quite different properties. As with most polymers, the form of the stress-strain curve will be highly dependent upon the test duration [2, 3] (visco-elasto-plastic behaviour).

Thus in order to make a complete analysis of the behaviour of such materials, it is important to have some measure of both the elastic and the plastic components as well as the time related properties. Indentation experiments, such as those we describe here, enable us to aquire such information, although the theory for the indentation of elasto-plastic materials by sharp indenters (semi-apical angle $\leqslant 50°$) is not complete: most of the relevant published work concentrates on the use of spherical or blunt pyramidal indenters [4–9]. Atkins and Tabor [10] using small angle cones pointed out that radial compression for such indenters would entail straining a large amount of material below the tip of the indenter. This, they argued, was more difficult to do, energetically, than "cutting and pushing sideways" as was actually observed using their model set-up. Thus the mode of deformation in this case corresponds to the slip-line deformation pattern rather than radial compression. Hirst and Howse [11] found likewise that radial compression was not observed and agreed also that rigid plastic behaviour does not occur for materials with a value of $(E/Y) \leqslant 100$ (PET has a value of $(E/Y) \approx 20$); thus PET falls into the class they term "complex elastic-plastic".

Previous work on polymers has tended to concentrate on the time-dependent properties. Grodzinskii [12] was the first to fully realize the potential of continuous depth recording during indentation tests and hence was able to monitor the time-dependent behaviour during both application and removal of load. Crawford [13] found that recovery of the indentation on unloading was mainly in the depth rather than the area of the impression. He also obtained an expression whereby, for a given material, a value of hardness can be calculated for any combination of loading time and load. An increase both in hardness and elastic recovery with increasing draw ratio to polyethylene fibres, as well as the effect on hardness of loading time, has been reported by Balta-Calleja [14, 15]. Finally, Darlix *et al.* [6, 7] analysed the time-dependent characteristics by the use of Maxwell and Voigt elements, allowing them to determine the strain and to derive values of Young's modulus (E) and yield stress (Y). The value of E is obtained from the recovery behaviour using Hertz's analysis of elastic contact. Y is then obtained via a measurement of depth corresponding to instantaneous elasto-plastic deformation using Studman's development [8] of an analysis derived by K. L. Johnson. They found broad agreement between the values obtained using their indentation tests and those obtained by more conventional methods. Several polymers were tested including polyethylene, and typical values for E were found to be ~ 1 GPa, with $Y \sim$ 10–100 MPa. Montmittonet

0022–2461/90 $03.00 + .12

(unpublished work) has since extended this work to include PET, and a value of ~5–6 GPa was obtained for E. In Kent's study of indentation processes in PMMA [4], he allowed for the variation of yield stress with time and hydrostatic pressure, using an expression of the form

$$Y = Y_0 + B \ln \dot{\varepsilon} + DP \quad (1)$$

where Y_0, B and D are constants dependent on material properties, $\dot{\varepsilon}$ is the radial strain rate, and P is the hydrostatic pressure. This equation is then used not to calculate Y, but to assign values to the ratio of the plastic zone radius/cavity radius for deep punching using a sphere. Experimental measurements of indentation pressure as a function of penetration rate, corrected for both elastic recovery and frictional effects, were compared with a theoretical prediction based on the expanding cavity model of Puttick *et al.* [5], using known values of the constants in Equation 1. Their values of indentation pressure ranged from 100 to 400 MPa (Y from 30 to 120 MPa).

In addition to abrupt load testing, we concentrate on the useful information which may be obtained via tests where the load is gradually increased and is then decreased once the desired maximum is reached. This type of slow loading "depth/load" test is particularly useful under conditions where the initial rapid elasto-plastic deformation is dominant. If continuous recording of data is used in conjunction with the depth–load measurement technique, elastic recovery as well as hardness as a function of depth can more readily be measured. van der Linden *et al.* [9] have recently measured the variation of viscoelastic properties of thin polyester/polyurethane layers as a function of TiO_2 pigment concentration. Otherwise, perhaps as a result of the technical difficulties involved, little work has been reported on fine-scale measurements, where the region of interest lies within a few microns of the polymer surface. This is the region that we are concerned with in this work. To eliminate, as far as possible, the effects of the bulk, we employ a pyramidal indenter with very small applied loads (0.02 to 15 mN). This gives a much smaller plastically deformed zone than is obtained with the more usual ball indentation method, and enables us to restrict the indented depth to less than 6 μm. Our aim was to assess the effect of a variety of fillers and of film drawing, by obtaining values of appropriate indices of plasticity and of elastic recovery [16] as a function of depth, thereby characterising the material, and, where possible, to derive values of material parameters such as Young's modulus.

2. Sample preparation and apparatus

For this work the polymer films were provided by Rhone-Poulenc Films and are listed in Table I. The fillers were incorporated in the form of "charges", to a concentration of between 2 and 15% by weight. The roughness (c.l.a.) was given as 50–700 nm, and it was noticed that several, perhaps all, of the samples had an apparent surface texture; even for the undrawn specimens, the texture appeared to show some degree of preferential alignment. The films were supplied in the form of A4 sized sheets from which we cut sections approximately 10 × 2 cm for mounting onto our specimen holders. Undrawn and uni-axially drawn films were glued onto metal holders using an epoxy resin, taking great care not to deform the film or touch the surface. We also attempted to test some biaxially drawn films, which were mounted using special holders designed to hold them flat: unfortunately, it has so far proved to be impracticable to mount these in such a way as to eliminate all air gaps between film and mount. Testing on these samples was, therefore, abandoned for the present.

TABLE I The polymer films

Sample	State	Filler	Thickness (μm)
10	Undrawn	Kaolinite	~300
20		TiO_2	
30		$CaCO_3$	
11	Uniaxially drawn	Kaolinite	~100
21		TiO_2	
31		$CaCO_3$	

As has been outlined previously, we were interested in the behaviour of the polymer films at less than ten microns depth and owing to their low resistance to penetration by a sharp indenter, this entails the use of an instrument capable of applying normal loads in the mN range. The instrument used is similar to that described recently [16], but with the electrostatic loading system replaced by an electromagnetic mechanism, enabling us to apply a higher maximum load, whilst retaining excellent low load capability. Briefly, the equipment comprises: a computer controlled stage, which moves the specimen between two positions, one for indenting and one for microscopic examination; a mechanism whereby the indenter movement is continuously monitored by computer via a capacitance bridge; and an electromagnetic loading device enabling tests at either constant load or constant loading rate to be performed at loads from 0.1 to 20 mN. The indenter diamond is a trigonal pyramid of apical angle 90°, so that the inevitable chisel point inherent in four-sided pyramids is avoided. Tests performed with a blunt indenter on a very hard and rigid sample confirm that at these very low loads, equipment compliance is negligible. The National Physical Laboratory recommends that if the effect of the substrate is to be negligible in the hardness testing of a film, the indentation depth should not exceed one tenth of the film thickness. Recent work by Lebouvier *et al.* [17, 18] indicates that, especially in the case of soft layers on a hard substrate, this criterion is too severe and that depths not exceeding one quarter of the film thickness may be acceptable. In fact in the experiments described here, the indentation depth was held below one tenth of the polymer thickness for both drawn and undrawn samples.

3. Slow loading ("depth/load") experiments

3.1. Experimental procedure

Before attempting tests where the indentation depth is measured as a function of slowly-varying load, it is

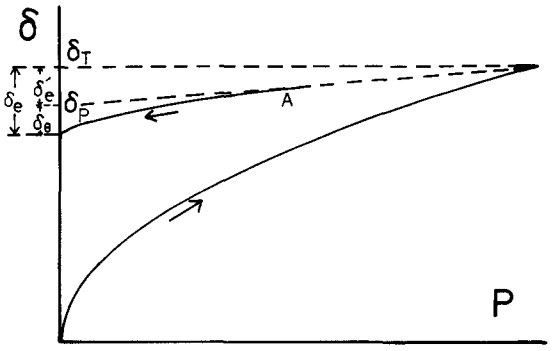

Figure 1 Depth (δ) as a function of load (P) (schematic).

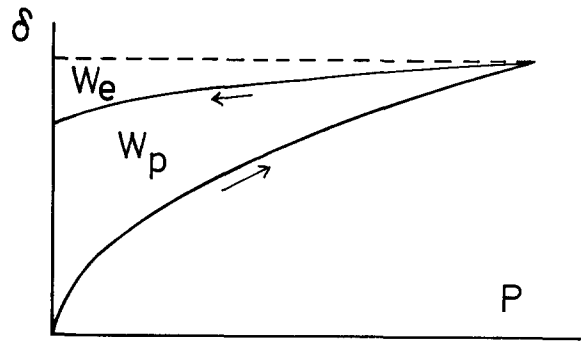

Figure 2 As Fig. 1, showing plastic and elastic work.

important to assess the degree of time-dependent behaviour for the material under test. Accordingly, we performed a short series of experiments at various loads which were held constant for a time comparable to the duration of the proposed ramping load tests. It was found that, for the polymers used here, 90% of the indentation depth was reached within 10 sec: we therefore chose a loading rate whereby the increase in load during a ten second period is only a small proportion of the maximum load of ~ 15 mN*.

A standardized procedure was used for all such tests, as follows:

(i) A fresh area of the film was located. This was generally at a lateral distance of ten times the indented depth from the last location.

(ii) Contact was made using an extremely small load, $\sim 3\,\mu$N, and immediately the loading cycle was commenced whereby the load increased at a rate of $0.11\,\text{mN sec}^{-1}$ until the desired maximum was reached. The load applied to the indenter and the indentation depth was monitored by computer throughout the experiment.

(iii) The load was decreased at the same rate, to zero.

(iv) The whole cycle was then repeated, but with a different maximum load in step (ii).

A great deal of care was taken to eliminate the effects of atypical regions where a scratch on the surface or a bubble below it were visible. As such imperfections were not always visible, we performed numerous tests on each sample, the data from which were then averaged and analysed by computer.

3.2. Separation of elastic and plastic contributions

Loubet *et al.* [19] have approached the problem of elasto-plastic indentation with the help of a simple approximation, namely that the total "on-load" elasto-plastic indentation depth delta δ_T may be expressed as the sum of plastic and elastic components δ_p and δ_e:

$$\delta_T = \delta_p + \delta_e \tag{2}$$

δ_p may thus be regarded as an "off-load" indentation depth. It is furthermore assumed that the area of contact between indenter and specimen is determined by the plastic deformation only, and that δ_e represents the movement of this area as a result of elastic deformation of the surrounding material. If this were exact, δ_e would be given by Sneddon's relation [20] for a flat cylindrical punch normally loaded onto the plane surface of a smooth elastic body:

$$P = \frac{2Ea\delta_e}{1 - \nu^2} \tag{3}$$

where P is the applied load, a is the radius of the contact region, E is Young's modulus and ν is Poisson's ratio (whose value here is taken as 0.5 [1]). Thus the unloading curve of δ as a function of P would be linear. In practice, there is some significant departure from linearity occurring after a certain point (A in Fig. 1). We have considered the possibility that this could indicate the type of plastic deformation arising from residual stresses during *unloading*. Such behaviour, possibly associated with crack behaviour, can occur in macroscopic experiments [21], but we find this departure from linearity at all loads. We attribute it to a decrease in contact area arising from an opening of the apical angle of the indent, and define a corrected value δ'_e to be used instead of δ_e in Equation 3. Since δ'_e may be determined experimentally, δ_p may be found from Equation 1 and it is possible therefore in principle to derive separate values of the appropriate parameters describing the elastic and plastic behaviour of the material. Two difficulties remain: the choice of a suitable elastic recovery parameter in the case of inhomogeneous materials; and the determination of the true zero of the indentation depth from which δ_p in particular is to be determined.

3.3. Work of indentation and choice of recovery parameter in the general case

Our definition of elastic recovery parameter R is

$$R = \frac{\delta'_e}{\delta_p} = \frac{\delta'_e}{\delta_T - \delta'_e} \tag{4}$$

(this definition is more logical than the one put forward previously [16]; in practice the difference is generally insignificant). From Equations 3 and 4 we see that for a homogeneous material, R is proportional to the ratio of hardness H to modulus $E/(1 - \nu^2)$, since $\delta_p^2 = \pi a^2/k_1$ where k_1 is the appropriate geometrical factor:

$$R = \frac{P(1 - \nu^2)}{2Ea} \frac{(k_1/\pi)^{1/2}}{a} \tag{5}$$

*Thereafter, for this type of test, we took the measured elastic component (δ_e) of the depth to represent the sum of instantaneous and delayed components. Later we describe how these may be distinguished.

but $H = P/\pi a^2$, giving

$$R = \frac{H(1 - \nu^2)(k_1\pi)^{1/2}}{2E} \quad (6)$$

However, the difficulty of determining δ_e' directly from the unloading curve, leads us to find an alternative method. The area under the depth–load curve is related to the work done by the indenter on the sample. By subtracting the area under the unloading curve from the total area, we measure the work retained by the sample. The nomenclature is given in Fig. 2. From this:

$$W_T = W_p + W_e$$

For an elastic material, all the work is released on unloading, i.e. $W_p = 0$ and $\delta_p = 0$. For a plastic material, all the work is retained by the sample, i.e. $W_p = W_T$ and $\delta_p = \delta_T$. In practice, the most precise way of characterising δ_e' is to re-define it from the released work W_e, using the same expression as applies for a perfectly linear unloading curve:

$$\delta_e' = 2W_e/P \quad (7)$$

In effect we neglect here the curve's departure from linearity, and also any residual elastic stresses remaining after unloading. Thus we have:

$$R = \left(\frac{P\delta_T}{2W_e} - 1\right)^{-1} \quad (8)$$

Our experimental results even for non-linear unloading curves show that, to within 5%:

$$\left(\frac{P\delta_T}{2W_e} - 1\right)^{-1} = \frac{\delta_e'}{\delta_p}$$

so that we regard Equation 8 as the most useful empirical expression for the elastic recovery parameter in the general case.

3.4. Determination of the true zero of the depth scale

Once values of R have been found for several different values of maximum load, the correction δ_e' is then subtracted from δ_T to give the plastic contribution δ_p. In general, factors such as noise and imperfect sharpness of the indenter make it difficult at times to determine where the zero of the scale of δ_p should be. Often however, δ_p is found to be proportional to the square root of load over a considerable load range, in which case the depth-zero is obtained by linear extrapolation of such a plot back to zero load. The result may be confirmed with the help of an alternative procedure: taking $W_T = \int P\,d\delta$ and assuming that P is proportional to δ_T^2, W_T is seen to vary as δ_T^3, so that a similar extrapolation to zero W, on a graph of $W^{1/3}$ against δ_T, will also give the depth-zero.

3.5. Plasticity indices and hardness

"True" hardness may be obtained only from measurement of the indent area. This process can prove imprecise even for standard microhardness tests (due to the small size and irregular shape of the indent) but, for the so-called "picohardness" region, the use of an electron microscope is often needed, with all the problems that entails. Absolute hardness values derived from tests on this scale are often suspect, and it may be more satisfactory to derive empirical indices of plasticity for comparing two or more different samples. Even this cautious approach may prove misleading if, as discussed recently by Chaudhri [22], the two samples have significantly different pile-up characteristics. We follow the procedure of Pollock *et al.* [16], where a correction is made for elastic recovery and then plasticity indices (relative hardnesses) are derived from the averaged curves of δ_p as a function of load:

$$I_p' = \left(\frac{dP^{1/2}}{d\delta_p}\right)^2$$

$$I_h' = \left(\frac{dP}{d(W^{2/3})}\right)^3$$

or, in non-differential form:

$$I_p = \frac{P}{\delta_p^2} \quad (9)$$

$$I_h = \frac{P^3}{W_p^2} \quad (10)$$

In the simplest case when δ_p is proportional to $P^{1/2}$ throughout we find:

$$I_h = 9I_p \quad (11)$$

and when the geometrical indenter constant k_1 has a value of 2.6:

$$H = I_p/2.6 = I_h/23 \quad (12)$$

If the elastic recovery is small, it may prove unnecessary to distinguish between δ_p and δ_T, in which case it is important to state that the resultant values of plasticity indices are on-load rather than off-load.

3.6. The shape of the elasto-plastic loading curve

In this section we first predict the simplest form of elasto-plastic loading curve (for which $P \propto \delta^2$); if it can be fitted well to the experimental loading data, a value of elastic modulus (E) is thereby obtained, independent of that derived from measurements of the elastic recovery parameter (Equation 6). If the fit is poor, we cannot assume that E is independent of depth, or that the $P \propto \delta^2$ law still applies. However, the more general empirical expression $P = k\delta^n$, together with a determination of the value of the exponent n, can still allow us to characterize the elasto-plastic behaviour of the material.

3.6.1. Determination of elastic modulus for homogeneous specimens (with n = 2)

We follow the analysis of Loubet *et al.* [19], the validity of which does not depend on the value of E/Y. It therefore should be valid for a wide variety of materials, including polymers. They assume that a uniform, homogeneous, elasto-plastic material with perfect plasticity will obey the expression

$$P = k_{ep}\delta_T^2 \quad (13)$$

where k_{ep} is an elasto-plastic constant which we may express in terms of H and $E/(1 - \nu^2)$. From Equation

2 and 4 we have:

$$\delta_T = \delta_p(1 + R)$$

Using the definition of hardness $H = P/\pi a^2$, the geometrical relation $\delta_p^2 = \pi a^2/k_1$, and Equation 6 which gives R in terms of H and E, we have:

$$\delta_T = \left(\frac{P}{k_1 H}\right)^{1/2}\left(1 + \frac{(\pi k_1)^{1/2}(1 - \nu^2)}{2E}\right)$$

Therefore,

$$k_{ep} = \frac{P}{\delta_T^2} = \left[\frac{1}{(k_1 H)^{1/2}} + \frac{\pi^{1/2}}{2}\frac{H^{1/2}(1 - \nu^2)}{E}\right]^{-2}$$

In the case of a 90° trigonal pyramid indenter, $k_1 = 2.6$ giving

$$k_{ep} = \left[\frac{0.62}{H^{1/2}} + \frac{0.89(1 - \nu^2)H^{1/2}}{E}\right]^{-2} \quad (14)$$

Thus if H is known, and either R (Equation 6 or 8) or k_{ep} (Equation 14) is measured, E may be calculated.

3.6.2. Determination of the exponent n in the general case

This exponent proves to be a useful parameter in situations where the values of R, E or H vary significantly with depth, which consequently no longer varies as $P^{1/2}$. An evaluation of n, which in practice lies between 1 and 3, may be made by use of a variety of techniques, usefully summarized by Loubet *et al.* [19]. Some are highly sensitive to electronic noise whilst others depend on a good degree of accuracy in the determination of the contact depth. An alternative technique we propose is to use the values of work obtained from the loading curve thus:

$$W_T = \int_0^{\delta_T} P\,d\delta = \frac{k_{ep}}{n + 1}\delta_T^{n+1}$$

Together with $P = k_{ep}\delta_T^n$ this gives

$$n = (P\delta_T/W_T) - 1 \quad (15)$$

The value of n thus derived is relatively unaffected by either noise or the accurate determination of the contact depth.

3.7. Results and discussion

Our objective was not so much to obtain absolute values, but more to compare one sample with another, thus establishing what effect different fillers may have and whether drawing affected the material properties. As we mentioned earlier, it proved impracticable to obtain reliable results on the biaxially drawn films, owing to the problems of mounting. Thus, no data for these samples will be presented here.

3.7.1. Microscopic examination

The indents produced by the application of a large load (e.g. 15 mN) were of the order of 10 μm across and thus visible under the microscope. It was immediately obvious that drawing the film had an effect on the indentation in that the triangular imprints left in the uniaxially drawn film were distorted, tending to be elongated in one or more directions, as observed by Balta-Calleja [15]. Sadly, the suppliers of the film could not inform us as to the draw direction, so we cannot relate the direction of drawing to this anisotropy. Also it was noted that the imprint was surrounded by visible wrinkling or piling-up, whose form was modified by the drawing of the film.

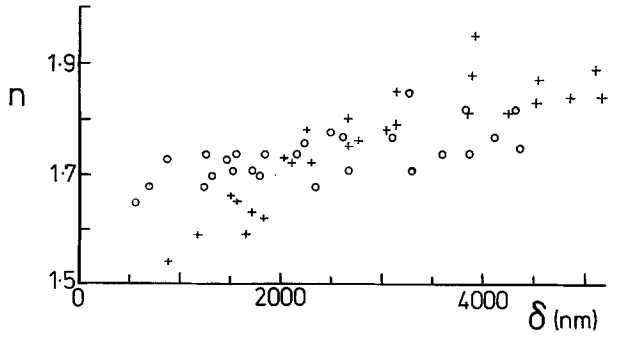

Figure 3 Depth-variation of the exponent n. Values for undrawn and uniaxially drawn PET are shown by crosses and circles respectively.

3.7.2. The exponent n

The most marked feature here is that the value of n, as measured using (15), varies in value between 1.5 and 1.9, the trend being to increase with increasing depth (Fig. 3). This indicates a mode of deformation more complex than previously supposed, thus limiting the validity of any equations where n is taken as equal to two or, indeed equations where $P = k\delta^n$ is assumed.

3.7.3. Plasticity indices

Figs 4–7 show data for both drawn and undrawn polymer films plotted in the form δ against $P^{1/2}$ and Ip, Ip′, or I_h against δ. Whilst a difference is detectable between the drawn and undrawn PET, no such distinction is noticeable between the samples containing different fillers; this suggests that most of the indents were made in between the filler charges and that the material sampled there was unaffected by their proximity. All four graphs demonstrate that an alteration in the surface mechanical properties takes place as a result of drawing, the greatest dichotomy being evident in Fig. 7, where the plasticity index I_h is plotted against the plastic penetration. Generally, we can say that the drawn films are harder than the undrawn and that the drawn films show a

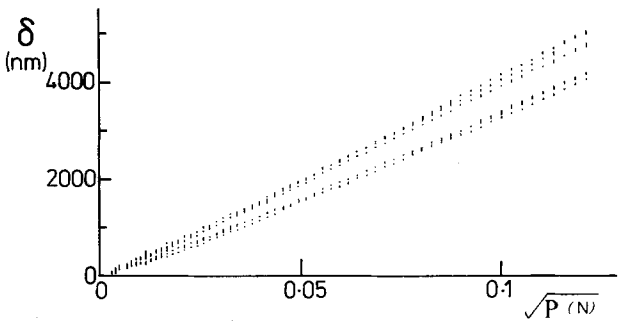

Figure 4 δ — $P^{1/2}$ data for PET: undrawn (upper curves) and uniaxially drawn (lower curves). Each vertical bar represents typically the average of between 5 and 50 data points. In the simplest case of a fully plastic material of constant hardness, the variation would be linear.

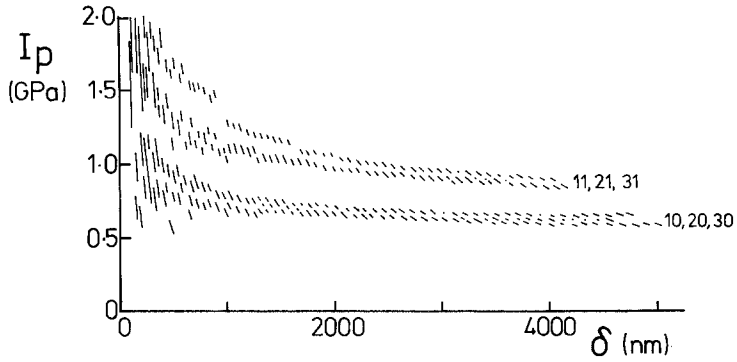

Figure 5 Plasticity index I_p as a function of δ_p, for the different sample numbers listed in Table I.

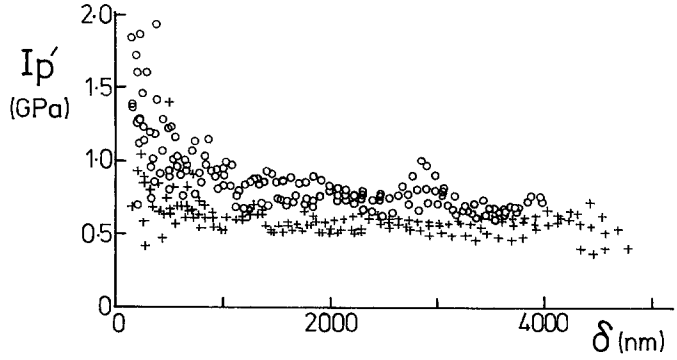

Figure 6 Differential plasticity index I'_p as a function of δ_p. Values for undrawn and uniaxially drawn PET are shown by crosses and circles respectively.

greater decrease in hardness as the indentation depth increases over the first few microns.

The explanation for this is not clear. Perhaps it is a manifestation of the "cutting" nature of the indentation process, with initial loading creating a small deflection of the surface, but with the polymer splitting along defects in the subsurface structure as the load increases. Alignment of the microfibrils during drawing would probably exaggerate this effect.

As stated previously (Equation 11), we should normally expect to find $I_h = 9I_p$ for a homogeneous specimen. Experiment indicates that, for these PET specimens, $I_h = 6I_p$ at the smallest depths and rises to $8I_p$ at larger depths. According to Equation 12, H is thus less than 0.5 GPa, although as discussed above it is inadvisable to rely upon an absolute value of hardness that is derived from depth measurements alone. An attempt was made to check this value of H using optical measurements of indent size: the accuracy was poor but the result was consistent.

3.7.4. Elastic Recovery

Again no significant difference is detectable between the samples containing different fillers. However, the elastic recovery parameter is a factor of two greater for the drawn samples compared with the undrawn (Fig. 8).

3.7.5. Evaluation of E

As explained earlier, even neglecting anisotropy we can only attempt to assign an effective value to the elastic modulus E (using Equations 6 and 14) if the hardness H and the recovery parameter R are independent of depth. From Figs 5 and 8 we can see that this is indeed the case for depths between 1 and 4–5 μm. At these large depths the value of 2.6 for the geometrical constant k_1 is regarded as reliable, so that Equation 12 may be used to eliminate H. Use of the recovery parameter in Equations 6 or 8 then gives us values of E equal to 3.0 GPa for the undrawn films and 2.4 GPa for the drawn; and, in practice, these are also the values which, when used in Equation 14, produce the best fit to the experimental depth–load curve (Fig. 9). In both cases the fit is good over the depth range given above. However, we point out that if it were possible to measure separately the moduli parallel to the directions of drawing and of indentation, then our conclusions as regards the decrease in modulus on drawing, might not always hold. The figures agree with the available literature, for example Bharat Bhusan [1] obtained a value of 2.7 GPa for PET film.

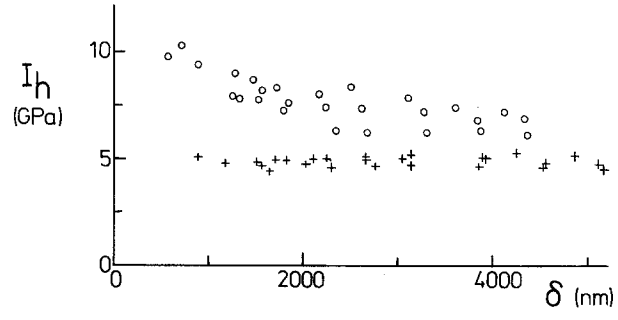

Figure 7 Hysteresis index I_h as a function of δ_p.

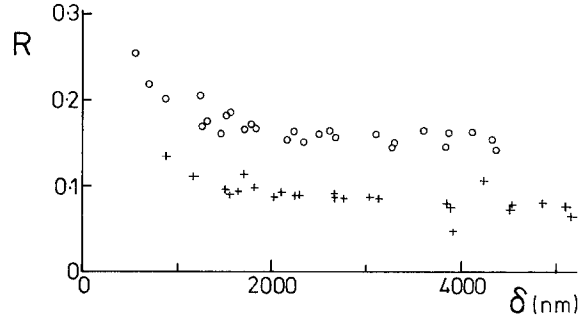

Figure 8 Elastic recovery parameter (R).

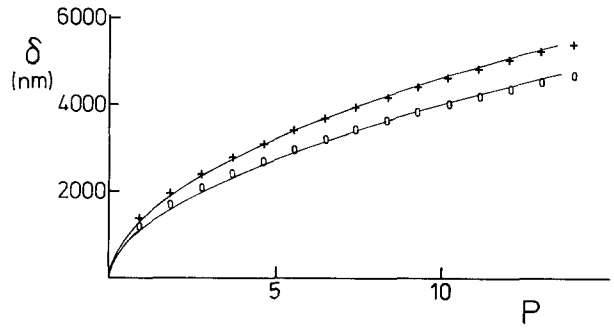

Figure 9 Agreement between experiment and theory (Equation 14) for depth-load curves: the values of elastic modulus E used for the fit are 3.0 GPa for PET 10 (undrawn: crosses) and 2.4 GPa for PET 11 (uniaxially drawn: circles).

4. Abrupt loading ("depth/time") experiments

4.1. Results

In the "δ–P" tests so far described, we chose a low rate of loading so that the measured elastic deformation would be close to its limiting value at infinite time. We now describe a series of "constant load" or δ–t tests, in which the load at the start was abruptly increased within less than a second to a chosen value, after which indentation depth was measured as a function of time, the measurement also being continued after the load had been suddenly reduced to zero. The purpose of these experiments was to investigate transient behaviour, which in principle might involve either retarded elasticity or visco-plastic (creep) effects. Clearly the initial stress was very much greater than in the δ–P tests, in that for more than a second, as the plastic and elastic zones grow, the indentation depth and area are relatively small. Under these conditions the behaviour of the PET showed several interesting features.

(i) The final plastic indentation depth was the same as in a slow loading (δ–P) test to the same maximum load (Fig. 10). However, the elastic recovery and the total maximum depth (elastic plus plastic) were greater (Figs 10 and 11). As shown later, this indicates that a very high transient initial stress level can lead to an increased total recoverable strain (at a given stress).

(ii) As expected, a marked anelasticity was seen. Here, the shape of the off-load curve was an exact inversion of that of the time-dependent part of the on-load curve (Fig. 12). This anelasticity did not however appear in tests where the indentation depth was very small (less than ~300 nm).

(iii) In general, any visco-*plastic* deformation was masked by the anelastic behaviour, as shown by the on-load/off-load symmetry just mentioned. However, at the smallest depths, where the anelasticity effectively disappeared and the observed loading curve was found to fit a simple viscoplastic formula, as shown in Section 4.5.

4.2. Discussion

We are not in a position to classify the behaviour of the polymer with the precision that is possible with the help of classical tensile testing techniques. Rather, we aim to show that the use of a pyramidal indenter allows us to detect different types of behaviour for polymer surfaces, on the basis of simple deformation models. In general we might expect one or more of the following types of visco-plastic behaviour.

1. Constant viscosity (η), i.e. plastic strain rate ($\dot{\varepsilon}_p$) proportional to stress (σ).

2. "Bingham" viscoplasticity, giving $\sigma - \sigma_0$ proportional to $(\dot{\varepsilon}_p)^n$, where σ_0 is a yield stress [23].

3. The model of Kent (see Equation 1) in which the yield stress varies with strain rate.

4. Other models by which either high strain rates [24] or longer times (thixotropy) lead to a lower effective viscosity.

In addition, possible types of behaviour involving time-dependent but *recoverable* (anelastic) deformation include

1. A power-law variation of elastic strain rate with stress [25].

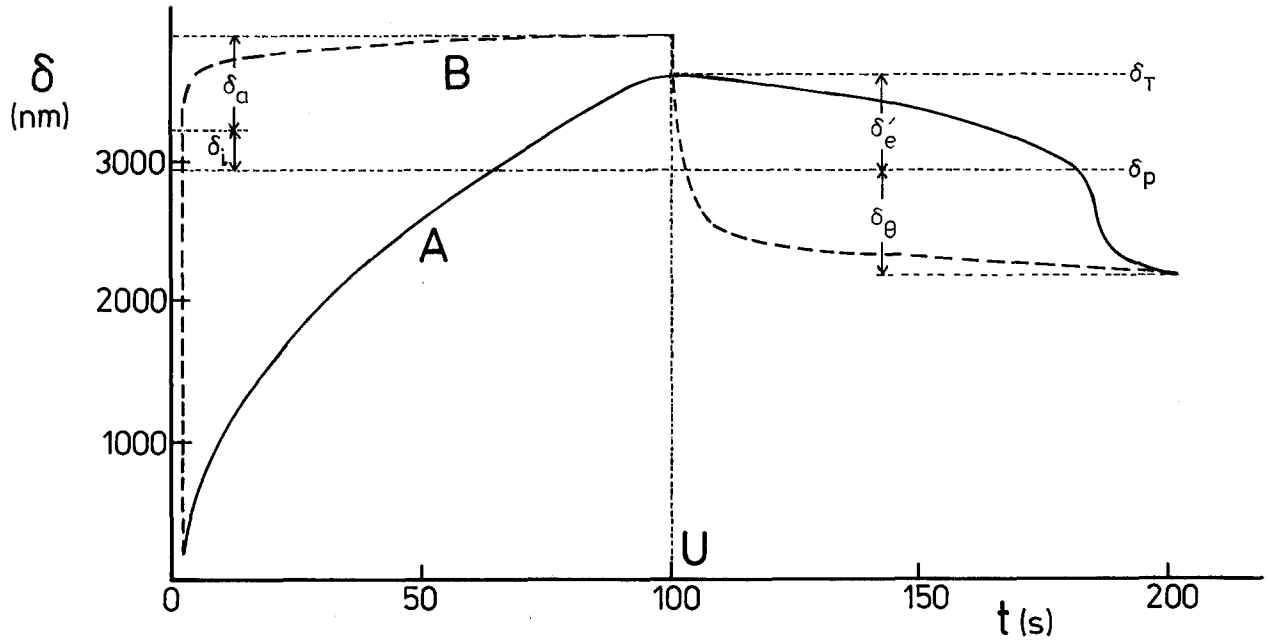

Figure 10 Indentation depth as a function of time, for (A) low rate of loading and unloading (0.08 mN sec^{-1}), (B) abrupt loading and unloading (symbols are defined in the text). Specimen: PET 21. (Maximum) load 7.8 mN and (onset of) unloading at 100 sec, in both cases.

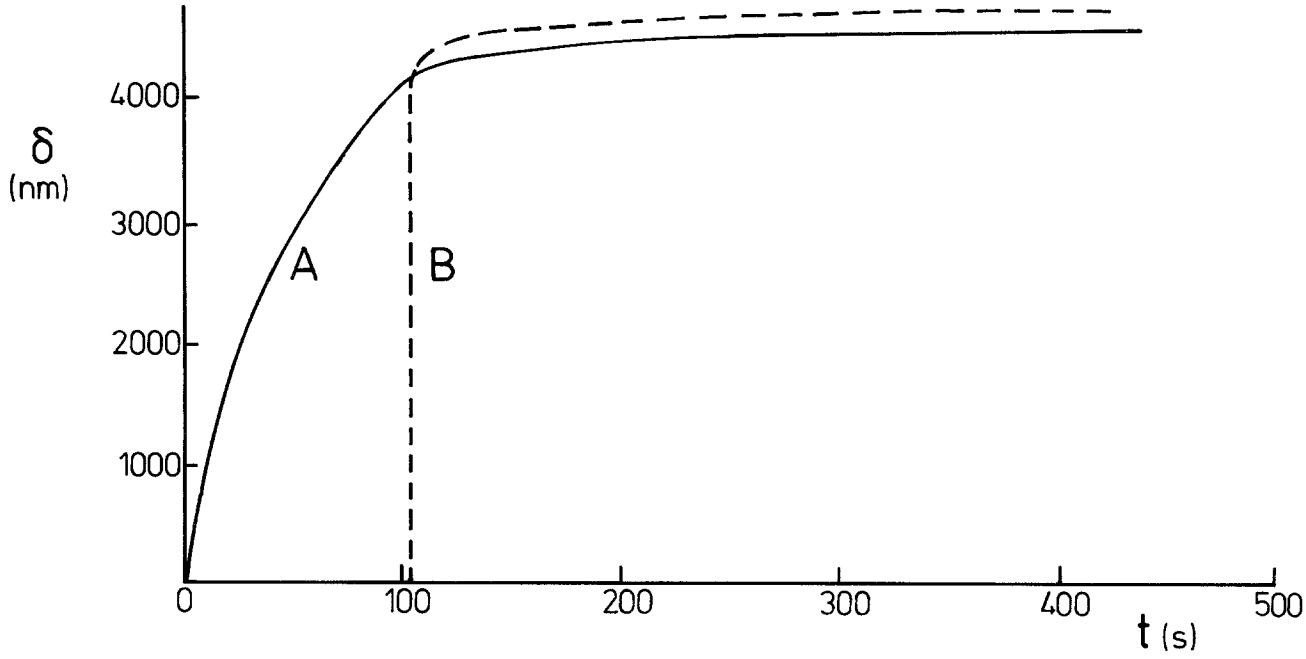

Figure 11 As Fig. 10, but undrawn PET (Sample 20), and showing the loading curve only. Note the significant difference in the final indentation depth at large t. A: loading rate 0.08 mN sec^{-1}; B: abrupt loading, same maximum load 8.37 mN.

2. Leathery behaviour (models of Maxwell, Voigt, Andrade, Trantina, Chasset ...), in which at a given stress, the elastic strain increases with time.

3. More complex models [26] in which stress is expressed in terms of (sometimes separable) functions of stress and time.

4.3. Relations between indentation depth, stress, strain, and strain rate

In our experiments as performed at present it is not possible to maintain a constant value of either stress or strain rate throughout a test. Following the assumptions described in an earlier review article [16], we make the following approximations.

1. Where the rate of increase of indentation depth ($\dot{\delta}$) is dominated by visco-plastic behaviour, then a simple description of the movement of the elastic/plastic boundary leads to the assumption that

$$\dot{\varepsilon}_p \propto \dot{\delta}/\delta \qquad (16)$$

We do not believe that plastic deformation is necessarily completed instantaneously even in a δ–t test.

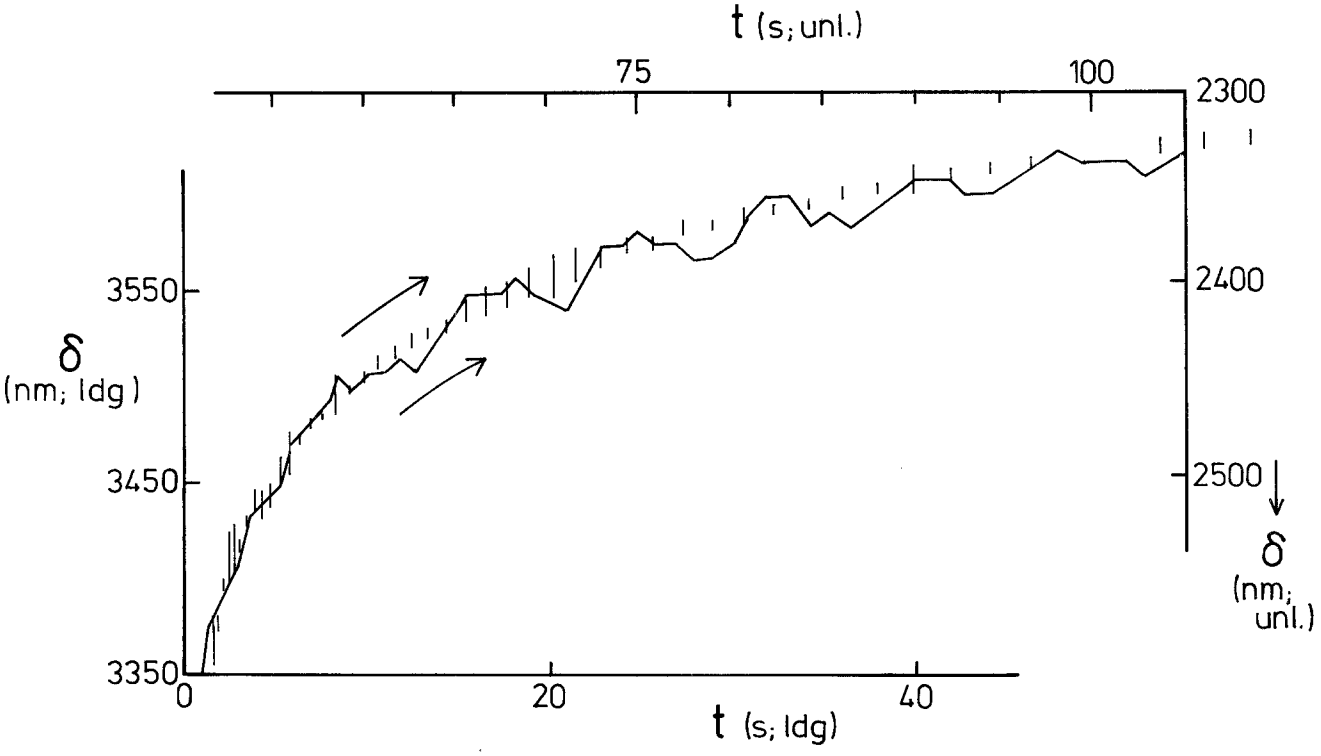

Figure 12 PET 20, abrupt loading (5.4 mN). The time-varying part of the off-load curve (shown upside down, continuous curve, right-hand and top scales) is an exact inversion of the on-load curve (vertical bars, left-hand and bottom scales), apart from an instantaneous relative displacement. (This is the sum of components δ_p, δ_i and δ_θ corresponding to plastic deformation, recovery in depth, and recovery in angle; see Fig. 10.)

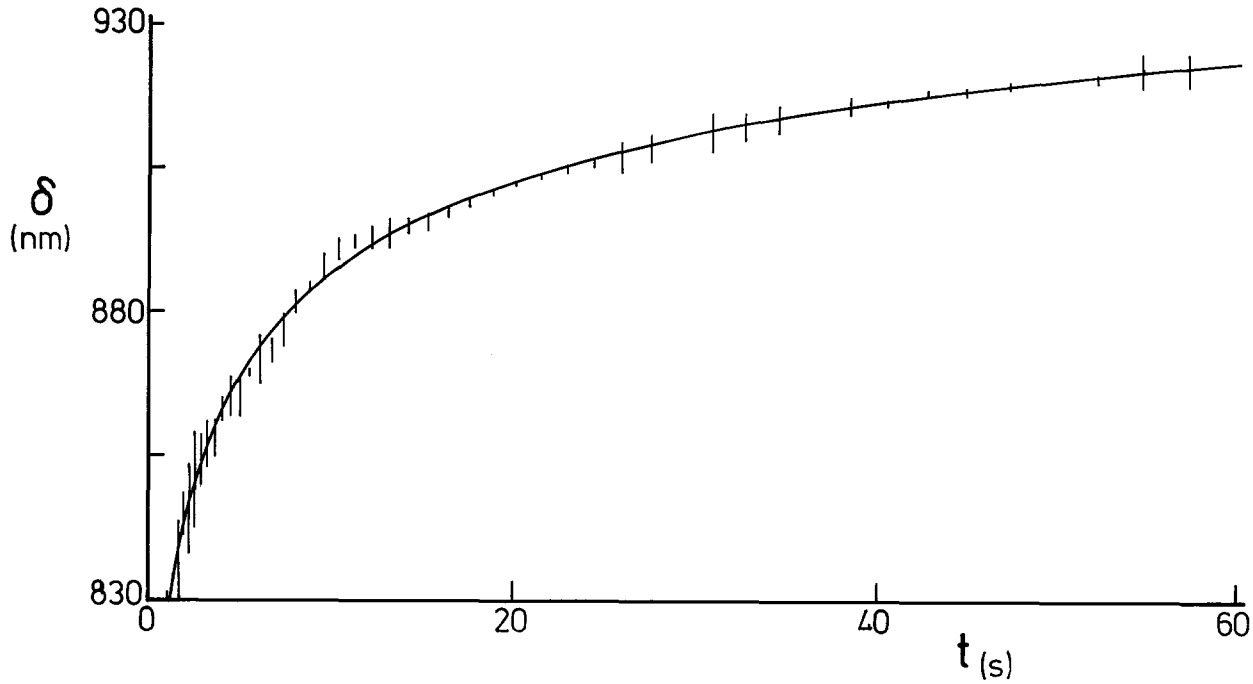

Figure 13 The Chasset formula (Equation 21) fitted to an "abrupt loading" curve (vertical bars) for PET 20 (load 0.4 mN), using the values $\delta_p + \delta_i = 745$ nm, $\delta_a = 218$ nm and $\tau = 3.0$ sec.

2. When plastic deformation appears to be complete, so that further changes in δ are dominated by elastic behaviour, then following the "flat-punch" argument summarized earlier (see Equation 3) we have:

$$\text{the elastic strain is proportional to } \delta_e \text{ at constant stress} \qquad (17)$$

3. From considerations of indenter geometry (compare Equation 9) we assume that stress is related to load and depth according to

$$\sigma \propto P/\delta_p^2 \qquad (18)$$

4.4. Anelastic behaviour

We have seen (Fig. 12) that at depths exceeding ~300 nm, the time-varying parts of the loading and unloading curves have the same shape. The deformation involved may thus be regarded as anelastic (recoverable), and could in principle be analysed in terms of the customary spring and dashpot model using Maxwell and Voigt elements. For our data, a much simpler analysis is possible if we use the empirical relation of Chasset [27]:

$$\text{compliance} \propto \frac{1}{1 + (\tau/t)^{0.5}} \qquad (19)$$

where τ is a constant*. Using Equation 17, and including an initial term $\delta_p + \delta_i$, then at constant P we have:

$$\delta = \delta_p + \delta_i + \frac{\delta_a}{1 + (\tau/t)^{0.5}} \qquad (20)$$

Of the two "instantaneous" components δ_p and δ_i, the first represents plastic deformation as before, while the second is elastic. δ_a is the recoverable but anelastic term. Fig. 13 shows an example of the excellent fit obtainable between Equation 20 and experimental data.

It is perhaps surprising that significant leathery behaviour is seen at room temperature, given that the glass transition temperature for PET is 90° C [29]. Tests performed so far have confirmed that this type of behaviour is seen for both amorphous and drawn PET, both indented to two different depths, namely 3000 and 700 nm. At the greater depth, the anelastic component gave a ratio δ_a/δ_p of 0.24 ± 0.01, the value of the time constant τ (Equation 20) being 4.0 ± 0.2 sec. The value of the instantaneous elastic component δ_i was given by $\delta_i/\delta_p = 0.06 \pm 0.01$, although the accuracy of this figure depends upon our assumption that δ_p is the same as in the slow loading tests (as suggested by the eventual joining-up of the two types of curve (see Fig. 10): the least accurately known parameter in this figure is the recovery in angle, δ_θ). At the smaller depth, the drawn material had a higher value of δ_i/δ_p while the amorphous material had a higher value of δ_a/δ_p: τ was 3.0 ± 0.5 sec. As suggested by Montmitonnet [21], it may be that the partly crystallized material has a retardation time spectrum that is shifted towards higher frequencies, so that part of the δ_a component becomes indistinguishable from σ_i.

To summarize the information on recoverable deformation:

1. In the slow loading rate (δ–P) tests, the drawn PET is found to have a lower modulus than the amorphous material, as judged by our technique which neglects anisotropy.

*If the exponent is treated as a second variable parameter instead of being given the value of 0.5 assumed here, Chasset's equation fits stress relaxation data for a range of lightly cross-linked polymers with a broad spectrum of relaxation times. It has no theoretical justification, but for relatively low testing frequencies is probably just as useful as the much more complex alternative models. A lower value of the exponent corresponds to increased elasticity, and the value of the time constant τ also depends upon the degree of cross-linking [28].

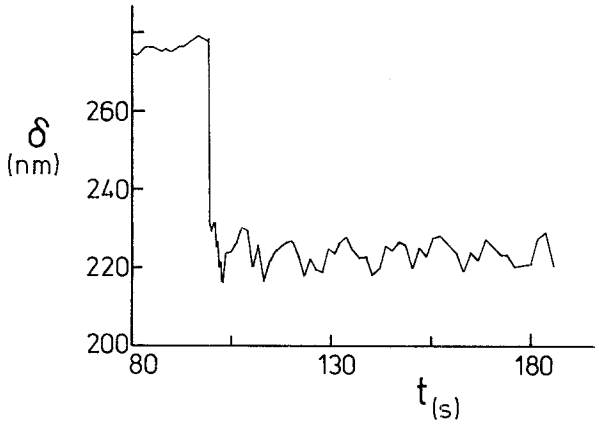

Figure 14 Abrupt unloading (PET 21) after (abrupt) indentation to small depth at a load of 0.041 mN. No time-dependent recovery is seen.

2. In the abrupt loading tests, in which we are able to separate the elastic and anelastic recoverable deformations, the total recoverable deformation is *greater*† than in the slow loading rate tests. This suggests that at the much higher mean stress involved in the abrupt loading tests, a detectable amount of viscous flow is occurring.

3. If we compare the ratios δ_a/δ_p and δ_i/δ_p with the values of recovery parameter δ_e'/δ_p in Fig. 8, we see that this increase in recoverable deformation seen with abrupt loading corresponds to the anelastic component: δ_a is much greater than δ_e'. This means that the previously observed difference in total elastic recovery between amorphous and drawn material is much less noticeable in these abrupt loading tests, where (except at the lowest depths) it is swamped by δ_a.

4. There is no detectable difference in the value of the anelastic time constant between the two materials.

4.5. Visco-plastic behaviour

In experiments where the load was small enough to give an indentation depth of less than 300 nm, no time-dependent recovery was detectable (Fig. 14). The reason for this is not clear, but the loading curve was analysed in accordance with the assumptions underlying Equations 16 and 18, and it was found that the strain rate varied as $(\sigma - \sigma_0)^{1/\eta}$ (see for example Fig. 15), where the value of the exponent $1/\eta$ was 5.2 for the amorphous and 2.6 for the drawn PET. This type of behaviour can be described as "Bingham" visco-plasticity, pseudoplastic ($\eta \leqslant 1$) rather than dilatant, the amorphous PET being closer to ideal plasticity ($\eta = 0$) than the drawn material. We have seen that as judged by the final plastic indentation depth for a given load, there was no detectable variation of yield stress with strain rate. This is not surprising, given that a decrease of only 20 per cent in *compressive* yield stress has been seen [29] between $\dot{\varepsilon} = 0.1$ and $\dot{\varepsilon} = 0.001$, and that in all our tests the strain rate finally falls to a very low value.

5. Conclusions

It is clear that useful information can be obtained by the use of indentation experiments on this scale. Seven main conclusions may be drawn from the work reported here:

1. Measurement of the indentation work provides us with a more reliable method of extracting information from the data than measurement of the total and recovered depths.

2. There is an indication that, especially for the drawn films, the relation $P = k\delta^2$ is not obeyed throughout the range of depths tested, the exponent n tending to increase as the depth increases, thus indi-

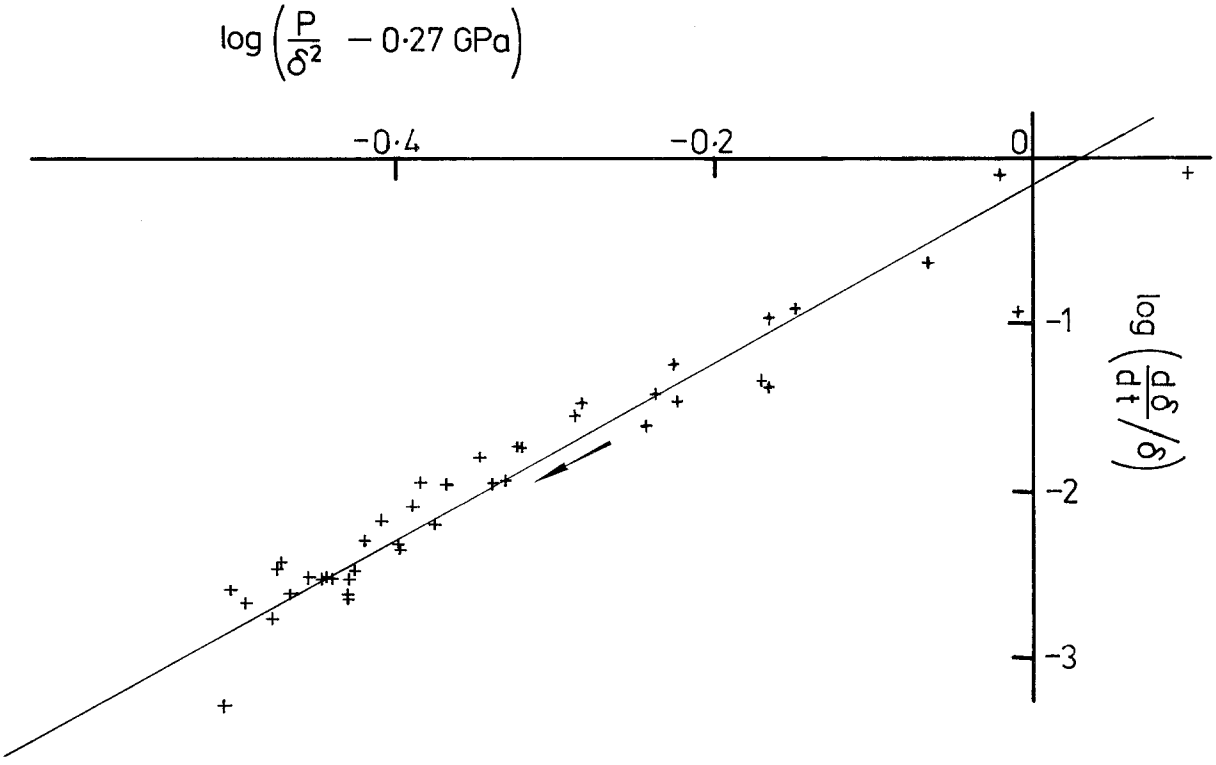

Figure 15 Small-depth abrupt loading data for amorphous PET (20) (load 0.021 mN), fitted to a simple visco-plastic formula.

† We note that since this additional depth is recoverable, it cannot be attributed to additional plastic deformation resulting from inertial effects.

cating that drawing the film has a pronounced effect on the topmost surface layers.

3. Visual observations of the remanent imprints indicate that the deformation mode for the drawn samples is markedly anisotropic.

4. We can use the data obtained from indentation experiments to obtain values for the Young's modulus of the material via two separate routes, both giving values of 1-3 GPa.

5. We have identified differences in both plasticity index and elastic recovery parameter between the drawn and undrawn samples: however, we found no evidence that the different filler materials had any effect upon the properties of the polymer in between the charges.

6. In the abrupt loading tests, the total recoverable deformation is greater, and includes an anelastic compliance that fits very well to a simple Chasset formula.

7. Indentations to very small depths ($\leqslant 300$ nm) allows us to detect pseudo-plastic loading behaviour, which is closer to ideal plasticity in the case of the amorphous material than with the drawn PET.

We therefore feel that indentation experiments on polymers, where special study is made of the top 10 μm or less, have a great deal of potential in the light of the growing use of such materials for critically designed components.

Acknowledgements

We are greatly indebted to Mr. T. Zajíček for performing exploratory measurements and to him, Dr M. M. Chaudhri, and Dr P. Montmitonnet for comments.

References

1. B. BHUSHAN and D. R. SMITH, *ASLE Trans.* **28** (1984) 325.
2. O. H. WYATT and D. DEW-HUGHES, "Metals, Ceramics and Polymers" (Cambridge University Press, 1974).
3. I. M. WARD, "Mechanical Properties of Solid Polymers", 2nd Edn (Wiley, New York, 1983).
4. R. J. KENT, *J. Phys. D, Appl. Phys.* **14** (1981) 601.
5. K. E. PUTTICK, L. S. A. SMITH and L. E. MILLER, *ibid.* **10** (1977) 617.
6. B. DARLIX, B. MONASSE and P. MONTMITONNET, *Polym. Testing* **6** (1986) 107.
7. B. DARLIX, P. MONTIMITONNET and B. MONASSE, *ibid.* **6** (1988) 189.
8. C. J. STUDMAN, M. A. MOORE and S. JONES, *J. Phys. D, Appl. Phys.* **9** (1976) 857.
9. J. H. M. VAN DER LINDEN, P. E. WIERENGA and E. P. HONIG, *J. Appl. Phys.* **62** (1987) 1613.
10. A. G. ATKINS and D. TABOR, *J. Mech. Phys. Solids* **13** (1965) 149.
11. W. HIRST and M. G. J. W. HOWSE, *Proc. R. Soc. A* **311** (1969) 429.
12. P. GRODZINSKI, *Plastics* (Sept. 1953) 312.
13. R. J. CRAWFORD, *Polym. Testing* **3** (1982) 37.
14. F. J. BALTA-CALLEJA, W. T. MEAD and R. S. PORTER, *Polym. Engng Sci.* **26** (1988) 393.
15. F. J. BALTA-CALLEJA, *Colloid Polym. Sci.* **254** (1976) 258.
16. H. M. POLLOCK, D. MAUGIS and M. BARQUINS, in "Microindentation Techniques in Materials Science and Engineering", edited by P. J. Blau and B. R. Lawn (ASTM STP 889, Philadelphia, 1986), p. 47.
17. D. LEBOUVIER, P. GILORMINI and E. FELDER, *J. Phys. D, Appl. Phys.* **18** (1985) 199.
18. J. C. PIVIN, D. LEBOUVIER, H. M. POLLOCK and E. FELDER, *ibid.* **22** (10) (1989) 1443.
19. J. L. LOUBET, J. M. GEORGES and G. MEILLE, in "Microindentation Techniques in Materials Science and Engineering", edited by P. J. Blau and B. R. Lawn (ASTM STP 889, Philadelphia USA, 1986) p. 72.
20. I. N. SNEDDON, *Proc. Camb. Phil. Soc.* **44** (1948) 429.
21. P. MONTMITONNET, DES Thesis, Ecole Nationale des Mines de Paris, Valbonne, France (1985); private communication (1988).
22. M. M. CHAUDHRI and M. WINTER, *J. Phys. D, Appl. Phys.* **21** (1988) 370.
23. J. HARRIS, "Rheology and non-Newtonian Flow" (Longman, London, 1977).
24. J. D. FERRY, "Viscoelastic Properties of Polymers", 3rd Edn (Wiley, New York, 1980), Ch. 1.
25. [24], Ch. 15.
26. [24], Ch. 6 and 14.
27. P. THIRION and R. CHASSET, *Chim. Ind. Gén. Chim.* **97** (1967) 617.
28. [24], Ch. 14.
29. R. A. DUCKETT, S. RABINOWITZ and I. M. WARD, *J. Mater. Sci.* **5** (1970) 909.

Received 19 January
and accepted 7 June 1989